APPLIED PHYSICS LETTERS 106, 142110 (2015)

Verification of electron doping in single-layer graphene due to H_2 exposure with thermoelectric power

Sung Ju Hong,[1] Min Park,[2] Hojin Kang,[1] Minwoo Lee,[3] David Soler-Delgado,[1] Dong Seok Shin,[4] Kyung Ho Kim,[1] Sergey Kubatkin,[5] Dae Hong Jeong,[3] Yung Woo Park,[1,a)] and Byung Hoon Kim[4,a)]

[1]*Department of Physics and Astronomy, Seoul National University, Seoul 151-747, South Korea*
[2]*Department of Nano Science and Technology, Seoul National University, Seoul 151-747, South Korea*
[3]*Department of Chemistry Education, Seoul National University, Seoul 151-742, South Korea*
[4]*Department of Physics, Incheon National University, Incheon 406-772, South Korea*
[5]*Department of Microtechnology and Nanoscience, Chalmers University of Technology, SE-412 96 Göteborg, Sweden*

(Received 25 February 2015; accepted 1 April 2015; published online 10 April 2015)

We report the electron doping of single-layer graphene (SLG) grown by chemical vapor deposition (CVD) by means of dissociative hydrogen adsorption. The transfer characteristic showed *n*-type doping behavior similar to that of mechanically exfoliated graphene. Furthermore, we studied the thermoelectric power (TEP) of CVD-grown SLG before and after exposure to high-pressure H_2 molecules. From the TEP results, which indicate the intrinsic electrical properties, we observed that the CVD-grown SLG is *n*-type doped without degradation of the quality after hydrogen adsorption. Finally, the electron doping was also verified by Raman spectroscopy. © *2015 AIP Publishing LLC*.
[http://dx.doi.org/10.1063/1.4917470]

Given that graphene, a two-dimensional honeycomb lattice of carbon, is an ideal monolayer, it has a large surface-area-to-volume ratio. Hence, charge transfer phenomena such as molecular sensing and doping have been extensively investigated.[1–8] We also recently reported *n*-type doping on graphene by dissociative hydrogen (H_2) adsorption.[9] The additional delocalized electron due to H_2 adsorption results in *n*-type doping, which allows the realization of lateral graphene *p*-*n* junctions.[10]

In order to utilize the *n*-type doping feature in applications, it is necessary to investigate the electrical properties of large-scale graphene such as single-layer graphene (SLG) grown by chemical vapor deposition (CVD). Furthermore, additional systematic and varied approaches are required to understand the electrical properties of CVD-grown SLG after exposure to H_2. (We denote this sample as SLG/H_2.) Revealing the electrical properties, the electrical resistance was mainly discussed in a previous report.[9] In addition to the resistance, thermoelectric power (TEP) and Raman spectroscopy can be used to explore electronic structures. The TEP, equivalent to the Seebeck coefficient S, is defined as $S = -\frac{\Delta V}{\Delta T}$, where ΔV and ΔT are the voltage and temperature difference through the sample, respectively. Because the TEP indicates the majority charge carrier in the system, this quantity is often adopted to probe charge transfer phenomena.[11–13] Raman spectroscopy is also a useful tool with which to probe the chemical potential and charge carrier interaction at the molecular scale.[14–18] Therefore, these two tools have been widely used to study charge-related phenomena in low-dimensional systems.

Here, we report the electrical properties, resistance, TEP, and Raman spectroscopy of CVD-grown SLG/H_2, which probe electron doping in a sample due to H_2 molecules. The Dirac point in the transfer curve, the resistance (R) vs the gate voltage (V_g), and the charge neutrality point (CNP) in the TEP shift to the negative V_g region. All of these findings are consistent with each other. From the simultaneous measurements of R and TEP, we found that the dissociated H_2-adsorbed graphene follows a semi-classical Mott relation and maintains an intrinsic electronic structure. Raman spectroscopy also provided the signature of electron doping in the carbon system. We proved that H_2 exposure contributes to electron doping manipulation.

Large-area SLG was grown on a copper foil (Alfa aesar 13382)[19] and transferred onto a 285 nm thick SiO_2 substrate.[20] Rectangular-shaped SLG (15 μm $\times$ 5 μm) was obtained by conventional electron beam lithography, followed by O_2 plasma etching. Finally, electrodes were fabricated by electron beam lithography and metal evaporation (Cr/Au = 5/50 nm). We designed a typical TEP measurement configuration which consists of a micro-heater, thermometers and a voltage probe, as shown in the inset of Fig. 1(a).[21] The two-probe resistance and TEP were simultaneously measured on the same device at 300 K in a vacuum and in a high-pressure H_2 atmosphere. The steady state TEP measurement was performed in the linear regime ($\Delta T \ll T$). We annealed the device at 390 K under a high vacuum ($\sim 5 \times 10^{-6}$ Torr) for 10 h for pristine SLG to remove residues in the high-vacuum/high-pressure chamber. The prepared SLG was exposed to a pressure of 11 bar of H_2 (99.9999%) at 350 K. Raman spectroscopy was carried out using a 532 nm laser with a power of 0.2 mW with a LabRam 300 by JY-Horiba.

Figure 1(a) shows the representative transfer curve of the CVD-grown SLG device. The black and blue curves correspond to SLG and SLG/H_2, respectively. We observed that the Dirac point shifted from 3.8 V to -0.6 V during the H_2

a)Authors to whom correspondence should be addressed. Electronic addresses: ywpark@phya.snu.ac.kr and kbh37@incheon.ac.kr

0003-6951/2015/106(14)/142110/4/$30.00 © 2015 AIP Publishing LLC

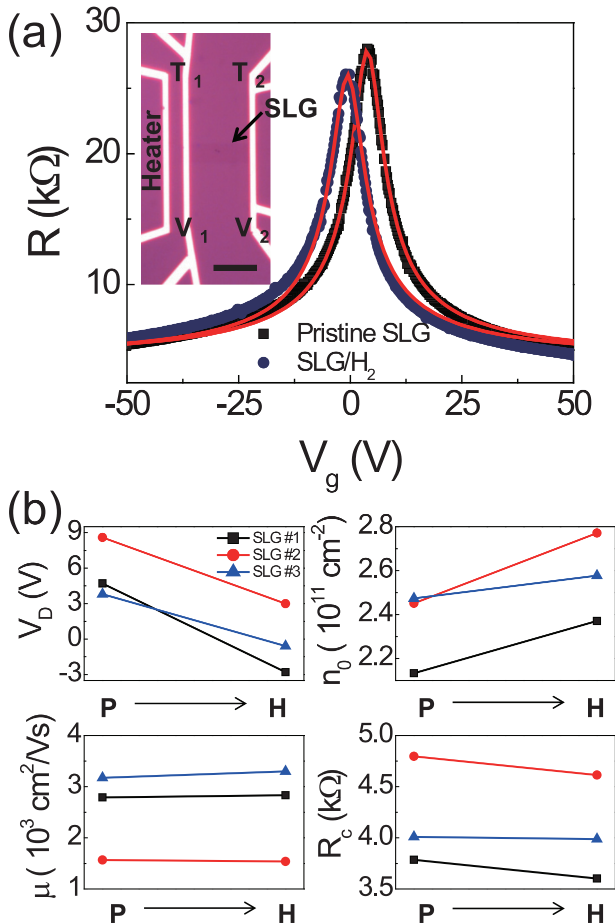

FIG. 1. (a) Transfer curves of pristine SLG (black) and SLG/H_2 (blue). The red lines are the fitting curves with the transfer curve model for SLG. The inset is an optical image of a typical configuration for the TEP measurement. The scale bar is 10 μm. (b) The fitting parameters (V_D: Dirac point, n_0: residual carrier density, μ: mobility, R_c: contact resistance) of pristine SLG (P) and SLG/H_2 (H) for three devices.

exposure process. *n*-type doping was previously reported and analyzed as a result of dissociative H_2 adsorption.[9] In order to analyze this more quantitatively, we fitted the result to the transfer curve model of SLG, $R = R_c + \frac{1}{e\mu}\left(\frac{L}{W}\right)\frac{1}{\sqrt{n^2+n_0^2}}$, where R_c, e, μ, L (W), n, and n_0 are the contact resistance, charge element, mobility, length (width), carrier density, and residual carrier density, respectively.[22] The carrier density was obtained from a two-parallel-capacitor model, $n = \alpha(V_g - V_D)$, where V_D is Dirac point and $\alpha_{SiO_2(285\,\mathrm{nm})} = 7.5\times10^{10}\mathrm{cm}^{-2}\,\mathrm{V}^{-1}$. The fitting parameters are presented in Fig. 1(b), showing a consistent tendency in the three devices. We found that the three devices are of a high quality with a mobility range of 1500–3500 $\mathrm{cm}^2\,\mathrm{V}^{-1}\,\mathrm{s}^{-1}$. The R_c and μ values are constant during the H_2 exposure process, while the n_0 value increases and the Dirac point shifts to the negative V_g region (from 3.8 V to -0.6 V). According to Kim *et al.*,[9] dissociative H_2-chemisorption affects the increase in the residual carrier density rather than the impurity density in SLG. This is in good agreement with our interpretation, which means that the residual carrier density increases but the mobility does not change after the H_2 exposure step. Because the residual carrier density is directly related to the resistance at the Dirac point, we can confirm that the experimental observation, R(SLG/H_2) $<$ R(SLG) at each Dirac point, is also valid.

With complement of the electrical resistance, the TEP can be used to study the intrinsic electrical properties. The TEP is sensitive to the electronic band structure and represents the entropy per unit charge.[21] Specifically, the TEP directly reveals the sign of the majority charge carrier of the system. We measured the TEP of both SLG and SLG/H_2 (Fig. 2(a)), which are symmetric with respect to TEP = 0 μV/K near the zero V_g. We observed a change in the CNP of the TEP from 4.1 V (SLG) to -0.7 V (SLG/H_2), which coincides with those of the Dirac points. These symmetric shape and coincidence between CNP and Dirac point indicate that the effect of defects such as wrinkles in CVD-grown SLG[23] is ignorable in this study. As typical behavior of the TEP, the sign of the TEP changes from positive (hole) to negative (electron) as V_g varies across the CNP. The TEP far from the CNP becomes zero, which can be understood by considering that the entropy per carrier decreases in a degenerate state, such as a highly doped regime. Quantitatively, it is known that SLG follows the semi-classical Mott relation, which is described by $S = -\frac{\pi^2 k_B^2 T}{3|e|}\frac{1}{G}\frac{dG}{dV_g}\frac{dV_g}{dE}\big|_{E=E_F}$, where k_B, T, G, and E_F are, respectively, the Boltzmann constant, the temperature, the conductance, and the Fermi energy. We also checked the Mott relation for the TEP of SLG and SLG/H_2, as shown in the upper and lower insets of Fig. 2(b), respectively. The measured TEPs are expressed with the black and blue curves, and the calculated TEP with the Mott relation

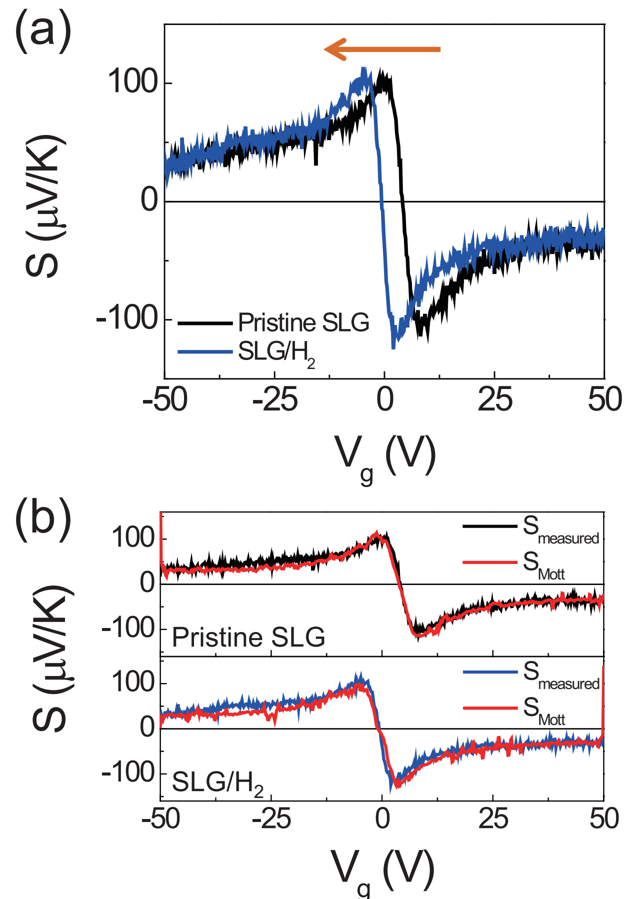

FIG. 2. (a) Measured TEPs of pristine SLG and SLG/H_2 as a function of V_g. (b) Comparison of the measured and simulated (the Mott relation) TEPs of pristine SLG and SLG/H_2.

This article is copyrighted as indicated in the article. Reuse of AIP content is subject to the terms at: http://scitation.aip.org/termsconditions. Downloaded to IP: 129.16.87.131 On: Thu, 09 Jul 2015 07:16:31

are presented using red curves for both cases. Given the consistency between the experimental and the calculated data, we observed that H_2-chemisorbed graphene as well as pristine graphene follow the semi-classical Mott relation. The TEP after H_2 exposure showed a simple position shift without distinctive shape deformation. In this light, we can conclude that the exposure of SLG to H_2 results in *n*-type doped graphene without a prominent change of the electronic structure.

n-type doping was also observed by Raman spectroscopy. The *G* and 2*D* peaks around 1580 cm^{-1} and 2700 cm^{-1}, respectively, are sensitive to the charge carrier density. For example, the position, the full width half maximum (FWHM) and the intensity ratio (I(2*D*)/I(*G*)) change depending on the doping.[14] In Fig. 3, we show the Raman spectra of SLG and SLG/H_2 in black and red lines, respectively. It was reported that a *D* peak around 1350 cm^{-1} appears and that C-H stretching mode at 2930 cm^{-1} develops in multilayer graphene after exposure to H_2.[9] In the CVD-grown SLG, there were no distinctive features for the *D* peak or the C-H mode, which is identical to results with mechanically exfoliated graphene. In contrast, it was clearly observed the change of the position, the FWHM and the I(2*D*)/I(*G*) as shown in the inset of Fig. 3. The positions of the *G* and *2D* peaks are correspondingly 1591 cm^{-1} (1582 cm^{-1}) and 2680 cm^{-1} (2674 cm^{-1}) for the pristine SLG (SLG/H_2). Both the *G* and the 2*D* peaks were red-shifted due to H_2 exposure. This can be understood by assuming that SLG is initially hole-doped. The *G* peak position non-monotonically depends on the carrier density; that is, the *G* peak position has a minimum at the Dirac point and increases with a higher carrier density regardless of the sign of the charge carrier.[14] On the other hand, the 2*D* peak is monotonically red-shifted when the majority carrier changes with an increase in the electron density. In addition, it was reported that the FWHM of the *G* peak is about 8 cm^{-1} and 16 cm^{-1} in a highly doped regime (holes and electrons) and at the Dirac point, respectively. The results in this study show that the FWHMs are 8 cm^{-1} for SLG and 15 cm^{-1} for SLG/H_2, which are in good agreement with earlier results.[14] This indicates that the pristine SLG is initially hole-doped and that the chemical potential of SLG/H_2 is closer to the Dirac point. Note that the FWHMs of the 2*D* peak are 25 cm^{-1} and 29 cm^{-1} for SLG and SLG/H_2, respectively. Moreover, I(2*D*)/I(*G*) changes from 1.3 to 2.5 after the H_2 treatment, which is also consistent with the findings in a previous report.[14] We noted that exfoliated SLG showed a Raman *G* peak blue-shift even in the hole carrier which was probed by transfer curve measurements.[9] A *d*-spacing study with transmission electron microscopy (TEM) revealed that the carbon lattice was compressed after H_2 exposure. Because the lattice strain as well as the charge carrier density affect the Raman spectrum, it is clear that the Raman spectrum results from the competition between these two factors.[24,25] Interestingly, two different strains, compressive and tensile strains, induce an opposite change in the Raman spectrum. For example, the *G* peak positions show a blue and red shift for compressive and tensile strain, respectively. Therefore, it is possible for exfoliated SLG to show a net blue shift, where the blue shift from the compressive lattice strains dominates the red shift from the electron doping.

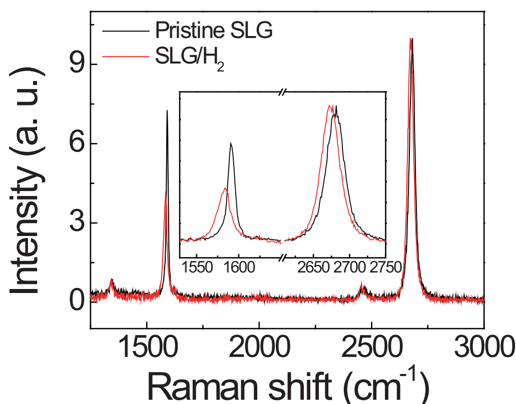

FIG. 3. Raman spectra of pristine SLG and SLG/H_2. The inset indicates the enlarged *G* and 2*D* peaks.

In summary, we fabricated CVD-grown SLG device and proved the electron doping by assessing the transfer characteristic and through TEP measurements and Raman spectroscopy. As an exfoliated sample, the CVD-grown SLG showed *n*-type doping after exposure to H_2. In particular, the TEP results show that H_2 exposure step induces *n*-type doping without any degradation in the quality. This study provides the easy means of electron doping manipulation in research fields associated with large-scale graphene.

This work was supported by the Leading Foreign Research Institute Recruitment Program (No. 2009-00514) of the NRF and by the FPRD of BK21 through the MEST, Korea. This research was partially supported from the Swedish-Korean Basic Research Cooperative Program (No. 2014R1A2A1A12067266) of the NRF, Korea. M.L. and D.H.J. acknowledge the support by the Pioneer Research Center Program through the NRF of Korea, funded by the Ministry of Science, ICT & Future Planning (No. NRF-2011-0027888). D.S.S. and B.H.K. acknowledge the support from the National Research Foundation of Korea (No. NRF-2014R1A1A1002467).

[1]F. Schedin, A. K. Geim, S. V. Morozov, E. W. Hill, P. Blake, M. I. Katsnelson, and K. S. Novoselov, Nat. Mater. **6**, 652 (2007).
[2]T. O. Wehling, K. S. Novoselov, S. V. Morozov, E. E. Vdovin, M. I. Katsnelson, A. K. Geim, and A. I. Lichtenstein, Nano Lett. **8**, 173 (2008).
[3]Y. Lu, B. R. Goldsmith, N. J. Kybert, and A. T. C. Johnson, Appl. Phys. Lett. **97**, 083107 (2010).
[4]P. L. Levesque, S. S. Sabri, C. M. Aguirre, J. Guillemette, M. Siaj, P. Desjardins, T. Szkopek, and R. Martel, Nano Lett. **11**, 132 (2011).
[5]Z. Luo, N. J. Pinto, Y. Davila, and A. T. C. Johnson, Appl. Phys. Lett. **100**, 253108 (2012).
[6]N. Cernetic, S. Wu, J. A. Davies, B. W. Krueger, D. O. Hutchins, X. Xu, H. Ma, and A. K.-Y. Jen, Adv. Funct. Mater. **24**, 3464 (2014).
[7]M. B. Lerner, F. Matsunaga, G. H. Han, S. J. Hong, J. Xi, A. Crook, J. M. Perez-Aguilar, Y. W. Park, J. G. Saven, R. Liu, and A. T. C. Johnson, Nano Lett. **14**, 2709 (2014).
[8]N. Liu, H. Tian, G. Schwartz, J. B.-H. Tok, T.-L. Ren, and Z. Bao, Nano Lett. **14**, 3702 (2014).
[9]B. H. Kim, S. J. Hong, S. J. Baek, H. Y. Jeong, N. Park, M. Lee, S. W. Lee, M. Park, S. W. Chu, H. S. Shin, J. Lim, J. C. Lee, Y. Jun, and Y. W. Park, Sci. Rep. **2**, 690 (2012).
[10]M. Park, Y. J. Yun, M. Lee, D. H. Jeong, Y. Jun, Y. W. Park, and B. H. Kim, AIP Adv. **5**, 017120 (2015).
[11]P. G. Collins, K. Bradley, M. Ishigami, and A. Zettl, Science **287**, 1801 (2000).

[12]Y. M. Choi, D. S. Lee, R. Czerw, P.-W. Chiu, N. Grobert, M. Terrones, M. Reyes-Reyes, H. Terrones, J.-C. Charlier, P. M. Ajayan, S. Roth, D. L. Carroll, and Y. W. Park, Nano Lett. **3**, 839 (2003).
[13]U. Dettlaff-Weglikowska, V. Skákalová, R. Graupner, S. H. Jhang, B. H. Kim, H. J. Lee, L. Ley, Y. W. Park, S. Berber, D. Tománek, and S. Roth, J. Am. Chem. Soc. **127**, 5125 (2005).
[14]A. Das, S. Pisana, B. Chakraborty, S. Piscanec, S. K. Saha, U. V. Waghmare, K. S. Novoselov, H. R. Krishnamurthy, A. K. Geim, A. C. Ferrari, and A. K. Sood, Nat. Nanotechnol. **3**, 210 (2008).
[15]S. Ryu, M. Y. Han, J. Maultzsch, T. F. Heinz, P. Kim, M. L. Steigerwald, and L. E. Brus, Nano Lett. **8**, 4597 (2008).
[16]A. Das, B. Chakraborty, S. Piscanec, S. Pisana, A. K. Sood, and A. C. Ferrari, Phys. Rev. B **79**, 155417 (2009).
[17]X. Dong, D. Fu, W. Fang, Y. Shi, P. Chen, and L.-J. Li, Small **5**, 1422 (2009).
[18]N. Jung, A. C. Crowther, N. Kim, P. Kim, and L. Brus, ACS Nano **4**, 7005 (2010).
[19]X. Li, W. Cai, J. An, S. Kim, J. Nah, D. Yang, R. Piner, A. Velamakanni, I. Jung, E. Tutuc, S. K. Banerjee, L. Colombo, and R. S. Ruoff, Science **324**, 1312 (2009).
[20]L. Gao, W. Ren, H. Xu, L. Jin, Z. Wang, T. Ma, L.-P. Ma, Z. Zhang, Q. Fu, L.-M. Peng, X. Bao, and H.-M. Cheng, Nat. Commun. **3**, 699 (2012).
[21]Y. M. Zuev, W. Chang, and P. Kim, Phys. Rev. Lett. **102**, 096807 (2009).
[22]S. Kim, J. Nah, I. Jo, D. Shahrjerdi, L. Colombo, Z. Yao, E. Tutuc, and S. K. Banerjee, Appl. Phys. Lett. **94**, 062107 (2009).
[23]Y. Nam, J. Sun, N. Lindvall, S. J. Yang, C. R. Park, Y. W. Park, and A. Yurgens, Appl. Phys. Lett. **104**, 021902 (2014).
[24]Z. H. Ni, H. M. Wang, Y. Ma, J. Kasim, Y. H. Wu, and Z. X. Shen, ACS Nano **2**, 1033 (2008).
[25]T. M. G. Mohiuddin, A. Lombardo, R. R. Nair, A. Bonetti, G. Savini, R. Jalil, N. Bonini, D. M. Basko, C. Galiotis, N. Marzari, K. S. Novoselov, A. K. Geim, and A. C. Ferrari, Phys. Rev. B **79**, 205433 (2009).